THE JOURNAL OF BIOLOGICAL CHEMISTRY Vol. 277, No. 2, Issue of January 11, pp. 1553–1559, 2002
Printed in U.S.A.

The β-Hairpin Motif of UvrB Is Essential for DNA Binding, Damage Processing, and UvrC-mediated Incisions*

Received for publication, September 13, 2001, and in revised form, October 24, 2001
Published, JBC Papers in Press, October 30, 2001, DOI 10.1074/jbc.M108847200

Milan Skorvaga‡§, Karsten Theis¶, Bhaskar S. Mandavilli‡, Caroline Kisker¶, and Bennett Van Houten‡‖

From the ‡Laboratory of Molecular Genetics, NIEHS, National Institutes of Health, Research Triangle Park, North Carolina 27709, §Department of Molecular Genetics, Cancer Research Institute, Slovak Academy of Sciences, Vlarska 7, 833 91 Bratislava, Slovakia, ¶Department of Pharmacological Sciences, Center for Structural Biology, State University of New York, Stony Brook, New York 11794-5115

UvrB plays a major role in recognition and processing of DNA lesions during nucleotide excision repair. The crystal structure of UvrB revealed a similar fold as found in monomeric DNA helicases. Homology modeling suggested that the β-hairpin motif of UvrB might be involved in DNA binding (Theis, K., Chen, P. J., Skorvaga, M., Van Houten, B., and Kisker, C. (1999) *EMBO J.* 18, 6899–6907). To determine a role of the β-hairpin of *Bacillus caldotenax* UvrB, we have constructed a deletion mutant, Δβh UvrB, which lacks residues Gln-97–Asp-112 of the β-hairpin. Δβh UvrB does not form a stable UvrB-DNA pre-incision complex and is inactive in UvrABC-mediated incision. However, Δβh UvrB is able to bind to UvrA and form a complex with UvrA and damaged DNA, competing with wild type UvrB. In addition, Δβh UvrB shows wild type-like ATPase activity in complex with UvrA that is stimulated by damaged DNA. In contrast to wild type UvrB, the ATPase activity of mutant UvrB does not lead to a destabilization of the damaged duplex. These results indicate that the conserved β-hairpin motif is a major factor in DNA binding.

Nucleotide excision repair (NER)[1] is a highly conserved DNA repair pathway found in bacteria, yeast, and man (1, 2). NER is remarkable because of the wide variety of chemically and structurally distinct DNA lesions that are substrates for this process (3). NER has been fully reconstituted from bacterial and mammalian proteins and can be viewed as four basic steps, damage recognition and processing, incision, repair synthesis, and ligation. One of the best-characterized NER systems is the UvrABC nuclease from *Escherichia coli* (4, 5). Repair by UvrABC is initiated when the trimeric complex of $UvrA_2B$ recognizes the damaged site. It has been suggested that the $UvrA_2B$ complex may locate damage through a limited helicase activity (6–8). However, more recent studies suggest that the strand-separating activity of the $UvrA_2B$ complex is not through a helicase-driven translocation step but in fact is due to local, relatively slow changes within the protein-DNA complex leading to a stable UvrB-DNA pre-incision complex and dissociation of the UvrA dimer (9–12). Once the UvrB-DNA complex has formed, UvrC, in what appears to be two different binding modes, first makes an incision four to five nucleotides 3′ to the modified nucleotide in an ATP-dependent step, which is followed by rapid incision seven nucleotides 5′ to the lesion in a step that does not require ATP hydrolysis (13). Recent work from Goosen and co-workers (14–17) strongly suggests, that in contrast to earlier reports (18, 19), UvrB has no intrinsic nuclease activity; 3′ incision is mediated by the N-terminal domain of UvrC and 5′ incision appears to be mediated by a nuclease center in the C-terminal domain of UvrC. After the incision reaction UvrD (helicase II) and DNA polymerase I are necessary and sufficient to release the excised oligonucleotide and allow UvrB and UvrC to participate in another round of incision (20, 21).

UvrB plays a central role in bacterial NER, participating in damage recognition, processing the DNA into a stable pre-incision complex, helping direct the activity of UvrC to perform the dual incisions, and finally staying bound to the non-damaged strand until being dislodged by DNA polymerase I (19, 22). UvrB contains six highly conserved sequence motifs, containing 10–40 amino acid residues each, that are found in all DNA helicases (23, 24). Three laboratories have independently solved the crystal structures of UvrB from thermophilic bacteria (25–28). UvrB is folded into five structural domains, 1a, 1b, 2, 3, and 4. The structure of domain 4, disordered in crystals of the full-length protein, has been determined separately (29). Domains 1a and 3 contain the six helicase motifs, placing UvrB as a member of the helicase superfamily II (30).

Superpositioning of UvrB onto other helicase structures has revealed that UvrB domains 1a and 3 are structurally closely related to the monomeric helicase fold found in PcrA, NS3, and Rep (28). Domains 1b and 2 are unique to UvrB, the latter being a binding site for UvrA. Comparing the structure of UvrB with these helicase structures revealed that UvrB contains all the structural properties of a helicase that couple ATP binding and hydrolysis to domain motions. However, if UvrB binds DNA in a similar manner as observed in the DNA complexes of these helicases, then the translocated DNA strand would be partially covered by a flexible β-hairpin structure. This unique structural element (see Figs. 1, *A* and *B*) connecting domains 1a and 1b was found to be highly conserved in all bacterial species. The β-hairpin is held in place with respect to domain 1b by two salt bridges and hydrophobic interactions at the base and the tip of the hairpin. Similar β-hairpin motifs found in PcrA and RNA polymerase II are thought to be essential for the strand opening performed by these two proteins (31, 32). We have previously shown that the DNA in the UvrB-DNA complex is

* This research was supported by grants from the Department of Energy and from the Pew Scholars Program in the Biomedical Sciences (to C. K.). The costs of publication of this article were defrayed in part by the payment of page charges. This article must therefore be hereby marked "*advertisement*" in accordance with 18 U.S.C. Section 1734 solely to indicate this fact.

‖ To whom correspondence should be addressed: NIEHS, P. O. Box 12233, MD D3-01, 111 T. W. Alexander Dr., Research Triangle Park, NC 27709. Tel.: 919-541-2799; E-mail: vanhout1@niehs.nih.gov.

[1] The abbreviations used are: NER, nucleotide excision repair; bp, base pair; dsDNA, double-stranded DNA; ssDNA, single-stranded DNA; wt, wild type.

partially melted over a 5-bp region (12). Based on these data, the UvrB structure, and comparisons to helicase structures and properties, a padlock binding mode for UvrB DNA interactions has been proposed in which UvrB wraps the β-hairpin around one DNA strand of partially unwound DNA in the pre-incision complex (25, 28). One critical test for this model is whether mutations in the β-hairpin affect binding and processing of damaged DNA.

Only one known mutation has been made in this motif, Glu-99 in UvrB (of *E. coli*), which was found to decrease the incision activity of the UvrABC system. To investigate the role of the β-hairpin motif in more detail, we constructed a β-hairpin mutant that replaced residues 97–112 with a glycine residue. We report here that this β-hairpin deletion mutant is greatly reduced in its ability to support incision, bind to a damaged containing duplex, and destabilize a damage containing 26-mer but has retained the ability to hydrolyze ATP in a UvrA- and damaged DNA-dependent manner. Thus, ATP hydrolysis and formation of the UvrB-DNA pre-incision complex are uncoupled in this mutant. The ability of the mutant to form a $UvrA_2B$-DNA complex and to hydrolyze ATP combined with its inability to form the UvrB-DNA pre-incision complex strongly suggests that the deleted residues are directly involved in DNA binding by UvrB.

MATERIALS AND METHODS

Enzymes—UvrA, UvrB, and UvrC proteins (Fig. 1*C*) from *Bacillus caldotenax* were purified by standard procedures (NEB IMPACT™ T7 system manual) with some modifications for each protein, which will be published elsewhere. T4 polynucleotide kinase was purchased from Life Technologies, Inc. *Pfu* DNA polymerase was purchased from Stratagene.

Construction of the β-Hairpin Deletion Mutant of UvrB—The deletion of amino acid residues Gln-97 to Asp-112 and introduction of a glycine residue in the deleted region constitutes the Δβh UvrB mutant. The *uvrB* gene has been subcloned into a pUC18 vector, and the construction of the mutant was performed by PCR using pUC18uvrB as a template DNA, db3 (5′-GCGAAAATCAACGATGAAATCGAC-3′) and db5 (′-GCCATAGTAATCGTAATAGCTGACAAATA-3′) oligonucleotides as PCR primers, and *Pfu* DNA polymerase using the QuikChange site-directed mutagenesis kit (Stratagene). The entire fragment amplified by PCR was sequenced to ensure that only the desired but no additional mutations were introduced.

DNA Substrates—Fluorescein-containing DNA substrates were synthesized by Sigma. The DNA sequence of a 50-bp dsDNA substrate containing a single internal fluorescein adduct (F_{26}-50 dsDNA) is shown in Fig. 2*A*. For 5′ labeling, 10 pmol of 50-mer fluorescein-containing top strand was incubated with 25 units of T4 polynucleotide kinase in 70 mM Tris/Cl (pH 7.6), 10 mM $MgCl_2$, 100 mM KCl, 1 mM 2-mercaptoethanol, and 15 pmol of [γ-^{32}P]ATP (3000 Ci/mmol). After incubation at 37 °C for 1 h, the reaction was terminated by incubation at 80 °C for 10 min in the presence of 20 mM EDTA. Annealing of the top and the bottom strand was performed in the presence of 50 mM NaCl followed by purification through Bio-Spin P-30 polyacrylamide gel column (Bio-Rad) for removal of unincorporated nucleotides. The double-stranded character and homogeneity of the 50-bp substrate were examined by a restriction assay (38) and analyzed on a 12% polyacrylamide sequencing gel under denaturating conditions.

The DNA sequence of the helicase substrate (HS1F-M13mp19) is shown in Fig. 2*B*. Five pmol of a 26-mer containing an internal fluorescein adduct (HS1F) were labeled at its 5′ terminus under the same conditions as the F_{26}-50 top strand. The helicase substrate was constructed by hybridizing 0.4 pmol of 5′-labeled HS1F oligonucleotide with equimolar amounts of M13mp19(+) strand (Life Technologies, Inc.) and purified as described above.

Gel Mobility Shift Assay—Binding reactions were performed with 2 nM DNA substrate (5′-^{32}P-labeled F_{26}-50 dsDNA), 20 nM *B. caldotenax* UvrA, and 60 nM *B. caldotenax* UvrB in 20 μl of UvrABC buffer (50 mM Tris/Cl (pH 7.5), 10 mM $MgCl_2$, 50 mM KCl, 1 mM ATP, 5 mM dithiothreitol) for 20 min at 55 °C. Glycerol was then added to the reaction (8%v/v), and the reaction mixture was loaded onto a 4% native polyacrylamide gel (80:1). The gel and the running buffer (89 mM Tris, 89 mM boric acid, 2 mM EDTA) contained 1 mM ATP and 10 mM $MgCl_2$. The electrophoresis was performed for 3 h at 100 V at room temperature. The gel was dried and exposed against Storage Phosphor Screen (Molecular Dynamics) overnight at room temperature.

UvrABC Incision Assay—The 5′ terminally labeled F_{26}-50 dsDNA substrate (2 nM) was incised by UvrABC (20 nM UvrA, 60 nM UvrB, 50 nM UvrC) in 20 μl of UvrABC buffer at 55 °C for 1 h. The reaction was terminated by adding EDTA (20 mM). The samples were denatured with formamide and heated to 90 °C for 5 min and then quick-chilled on ice. The incision products were analyzed by electrophoresis on a 12% polyacrylamide sequencing gel under denaturating conditions at 400–600 V with Tris-borate-EDTA buffer. In the case of the helicase substrate incision, the reaction mixture (15 μl) contained ~8 fmol (in ssDNA circles) of DNA substrate, 50 nM UvrA, 100 nM UvrB, and 100 nM UvrC in buffer A2 (50 mM Tris/Cl (pH 7.5), 100 mM KCl, 15 mM $MgCl_2$, 1 mM EDTA, 5 mM ATP, 2 mM dithiothreitol) and was incubated at 42 °C for 1 h. The reaction was quenched with 5 μl of stop solution (25% (v/v) Ficoll, 1% SDS, 0.1 mM EDTA, 0.25% orange G) and heated for 2 min at 85 °C, and the entire sample was then loaded onto a 15% denaturating polyacrylamide gel equilibrated with Tris-borate EDTA running buffer. Electrophoresis was carried out at 400–600 V for 1–2 h. The gels were processed as described above.

CD Spectroscopy—CD spectra were measured at 20 °C on an Aviv model 62 ADS spectrometer using rectangular cells with a path length of 0.2 mm. Proteins were measured at concentrations between 0.6 and 1.4 mg/ml in a buffer containing 500 mM KF and 10 mM K_2HPO_4 at pH 7.4. UV absorption at 280 nm was used to determine protein concentrations. The extinction coefficients of wild type UvrB (658 amino acids) and UvrBΔβh (643 amino acids) were calculated from the primary sequence to be 33,280 and 30,720 liters/mol/cm, respectively. The CD spectra were sampled at 1-nm intervals with a time constant of 1 s and 10 scans for both samples and blanks, resulting in an acquisition time of 1 h for each spectrum.

Oligonucleotide-releasing Assay—The reaction mixture contained 50 nM UvrA, 100 nM UvrB, and ~8 fmol (in ssDNA circles) of helicase substrate (HS1F-M13mp19) in buffer A1 (50 mM Tris/Cl (pH 7.5), 150 mM NaCl, 10 mM $MgCl_2$, 2 mM ATP, 5 mM dithiothreitol) and was incubated at 37 °C for various time intervals. The reaction was stopped with 5 μl of stop solution (50% (v/v) glycerol, 1% SDS, 0.1 M EDTA, 0.25% orange G), and the entire sample was loaded on 12% non-denaturating acrylamide gel in Tris-borate EDTA running buffer. Electrophoresis was run at 120–150 V for 1–2 h, and the gels were processed as described previously.

ATP Hydrolysis Assay—The conversion of ATP to ADP by the UvrABC system was determined by a coupled enzyme assay system consisting of pyruvate kinase and lactate dehydrogenase to link the hydrolysis of ATP to the oxidation of NADH. The assay mixture consisted of 50 mM Tris/Cl (pH 7.5), 50 mM NaCl, 4 mM $MgCl_2$, 1 mM dithiothreitol, 20 units/ml lactate dehydrogenase, 20 units/ml pyruvate kinase, 2 mM phosphoenol pyruvate, 0.15 mM NADH and 200 nM Uvr proteins in the presence or absence of 50 ng of UV-irradiated DNA substrate. DNA substrate was prepared by exposure of pUC18 DNA to 200 J/m^2. *B. caldotenax* UvrA, UvrB, and UvrC proteins were preheated to 55 °C for 10 min to inactivate *E. coli* contaminant protein activities. The reaction mixture (0.5 ml) was allowed to equilibrate at 37 °C, and the assay was initiated by the addition of ATP (0.5 mM). The rate of ATP hydrolysis was calculated from the linear change in absorbance at λ = 340 nm over 30 min, which accompanied the oxidation of NADH, using a Beckman spectrophotometer. Determinations were performed in duplicate and done three separate times. Data are reported as the means ± S.D.

RESULTS

To test our padlock DNA binding model and the importance of the β-hairpin motif in the recognition of DNA damage, we have constructed a β-hairpin deletion mutant of the *B. caldotenax* UvrB protein, designed as Δβh UvrB, with amino acid residues from Gln97 to Asp112 removed and the resulting gap bridged by a glycine residue (Fig. 1, *A* and *B*). In the resulting deletion mutant only the upper half of the β-hairpin was removed. To test the properties of this mutant, we reconstituted the *B. caldotenax* UvrABC nuclease system with purified UvrA, UvrB, and UvrC (Fig. 1*C*), each obtained via intein fusion proteins.

UvrABC-mediated Incision of a Fluorescein-containing 50-bp Duplex Using the UvrB β-Hairpin Deletion Mutant—We first investigated the effect of Δβh UvrB on UvrABC endonuclease

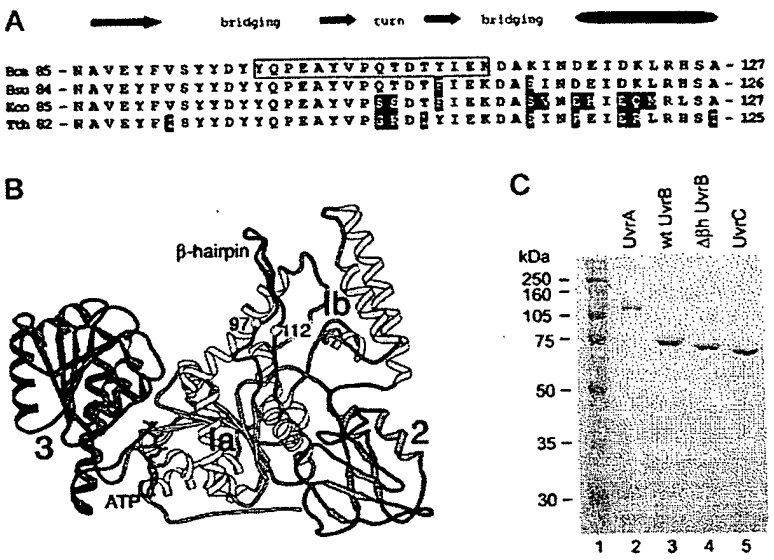

FIG. 1. **Construction of the UvrB β-hairpin deletion mutant (Δβh UvrB).** *Panel A*, alignments of UvrB proteins from *B. caldotenax* (*Bca*), *Bacillus subtilis* (*Bsu*), *E. coli* (*Eco*), and *Thermus thermophilus* (*Tth*). At each position, residues other than those present in *B. caldotenax* UvrB are *highlighted*. The amino acid residues deleted in Δβh UvrB are shown in a *box*. *Panel B*, location of the β-hairpin (*darkest shading*) in the three-dimensional structure of UvrB. In the deletion mutant, Δβh UvrB, residues Gln-97–Asp-112 have been replaced with a glycine. Gln-97 and Asp-112 are indicated by spheres in this ribbon diagram. *Panel C*, SDS-PAGE gel showing purified UvrA, UvrB, Δβh UvrB, and UvrC from *B. caldotenax*.

mediated-incision. The substrate was a 50-bp duplex containing a fluorescein moiety in the middle of the top strand (position F_{26}, see Fig. 2*A*), labeled at its 5′ terminus with [γ-^{32}P]ATP. Results of the UvrABC endonuclease incision kinetics of F_{26}-50 dsDNA are shown in Fig. 3. *Panel A* contains data for wild type UvrB, *panel B* contains data for Δβh UvrB, and *panel C* summarizes the incision kinetics. The results show that Δβh UvrB does not support UvrABC-mediated incision of substrate DNA. The residual incision of ≤5–6% represents the level of background for the substrate used. Clearly, deleting the β-hairpin of UvrB disrupts one of the steps that lead to incision of the damaged DNA.

Loading of the Δβh UvrB Protein onto the Site of Damage—The failure of Δβh UvrB to confer endonuclease activity to the UvrABC system might be due to failure to recognize the damage or failure to incise the damage after successful recognition. We used a gel mobility shift assay to test whether the intermediate between these processes, the UvrB-DNA pre-incision complex, is formed with the Δβh UvrB mutant (Figs. 4 and 5). The Δβh UvrB protein does not form a stable complex with the damaged DNA neither at low concentrations (1–20 nM; Fig. 4*A*) nor at higher amounts (50–200 nM; Fig. 4*B*), whereas loading of wild type UvrB is very efficient, even at 5 nM (Fig. 4*A*, *lane 7*). It is interesting to note that the band corresponding to the $UvrA_2$-DNA complex (Fig. 4*B*, *lane 2*) migrates slightly faster than the samples containing the Δβh UvrB protein (Fig. 4*B*, *lanes 4–6*). This slower mobility band probably represents the $UvrA_2$Δβh UvrB-DNA complex. To further investigate whether Δβh UvrB is able to bind to UvrA, we have conducted competition experiments between the mutant and the wild type UvrB for binding to UvrA and F_{26}-50 dsDNA. In these experiments (Fig. 5) there is a clear difference in mobility between the $UvrA_2$-DNA and $UvrA_2$Δβh UvrB-DNA complexes (Fig. 5, compare *lane 2* with *lanes 3–5*). Increasing amounts of Δβh UvrB (10, 50, 100 nM) at a constant wild type UvrB concentration (5 nM) resulted in a significant reduction of the amount of wt UvrB-DNA complex (Fig. 5, *lanes 4–6 versus lane 8*). This dominant negative effect of Δβh UvrB supports the idea that Δβh UvrB is properly folded and shows that it is capable of interacting with UvrA, resulting in the reduction of the amount of UvrA molecules available to interact with wild type UvrB.

CD Spectra of Wild Type and the β-Hairpin Deletion Mutant UvrB—Fig. 6 shows CD spectra of wild type (*filled ovals*) and Δβh (*open ovals*) UvrB proteins, respectively. The results exhibit nearly identical CD spectra for both wild type and mutant proteins, indicating that the deletion of the β-hairpin motif in UvrB does not affect the global folding of the protein.

Strand Destabilizing Activity of Δβh UvrB—In our padlock DNA binding model, we proposed that the β-hairpin of UvrB requires at least 5 base pairs of DNA to be disrupted so that the β-hairpin could be inserted between the strands of DNA. The limited strand opening by the $UvrA_2B$ complex has been shown previously to be important for dynamic recognition of DNA damage (11, 12) and has been called a limited helicase activity (6, 7). To evaluate the importance of the β-hairpin motif for the presumed helicase activity of the $UvrA_2B$ complex, we assayed Δβh UvrB in a strand destabilization assay that measures the release of a radioactively labeled 26-mer containing fluorescein annealed to a single-stranded DNA circle (M13mp19(+) strand). The results are shown in Fig. 7, with kinetics of the 26-mer release summarized in *panel C*. Although wild type UvrB supports the release of the fluorescein-containing 26-mer very efficiently, reaching about 80% release of oligomer after 60 min, the β-hairpin deletion mutant has very low, if any, activity. It is critical to realize that the "release" of the oligomer is assayed after the addition of a stop buffer containing1% SDS and 0.1 M EDTA.

Incision of Strand-destabilizing Substrate by Δβh UvrB—If UvrB is capable of true strand displacement like a *bona fide* helicase, then the displaced strand would be single-stranded. However, single-stranded damaged DNA is not a substrate for the UvrABC system. As can be clearly seen in Fig. 7*D*, the helix-destabilizing substrate, a 5′-labeled 26-mer containing a fluorescein adduct annealed to M13mp19 ssDNA, was incised by the UvrABC nuclease system. The incision efficiency supported by wild type UvrB was ~55% (at 42 °C for 1 h; Fig. 7, *panel D*, *lane 2*), whereas the Δβh UvrB mutant did not support any incision of the 26-mer-fluorescein/M13 substrate. Based on this incision of the strand-displacement substrate with wild type UvrB (as part of the UvrABC endonuclease), we suggest that $UvrA_2B$ does not completely release the damage-containing 26-mer from a ssDNA circle until SDS is added as part of the stop buffer. Therefore, we feel it is inappropriate to call this activity a true helicase, and we suggest it is better to call this property of $UvrA_2$UvrB a strand-destabilizing activity.

ATPase Activity of Δβh UvrB—It has been shown previously

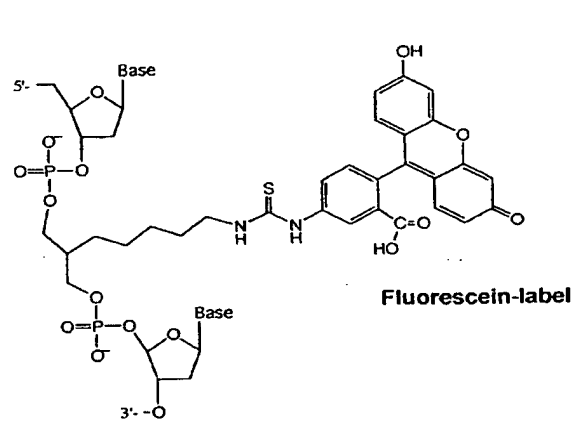

Fluorescein-labeled 50mer duplex

RsaI HaeIII

5' - GACTACGTACTGTTACGGCTCCATCFCTACCGCAATCAGGCCAGATCTGC - 5'
3' - CTGATGCATGACAATGCCGAGGTAGCGATGGCGTTAGTCCGGTCTAGACG - 3'

where F_{26} = internal fluorescein-label

FIG. 2. DNA substrates used in this study. *Panel A*, F_{26}-50 dsDNA substrate, 50-base pair duplex with fluorescein attached at position 26. *Panel B*, schematic representation of the helicase substrate, HS1F-M13mp19(+). The figure shows the complete nucleotide sequence of a fluorescein-containing 26-mer (*bottom strand*), HS1F, that has been annealed to single-stranded M13mp19(+) DNA (*top strand*). The position of the fluorescein adduct in the bottom strand is designated as a *bold F*.

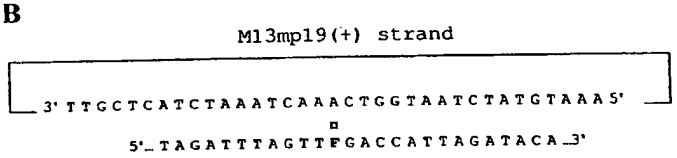

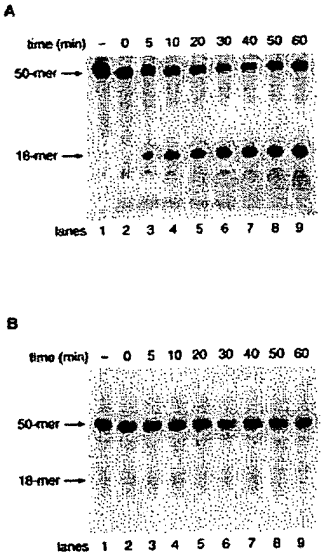

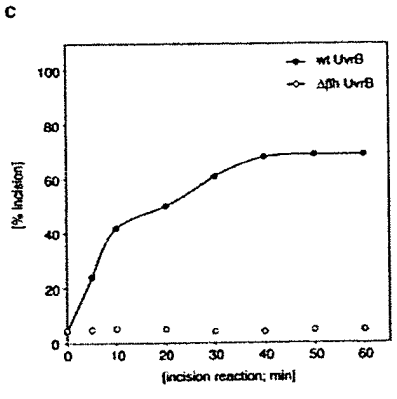

FIG. 3. **ΔβhUvrB does not support incision of a fluorescein containing a 50-bp duplex.** The F_{26}-50 dsDNA substrate (2 nM) (sequence shown in Fig. 2*A* with a 5' terminally labeled modified strand) was incubated with UvrA (20 nM), UvrB (60 nM), and UvrC (50 nM) at 55 °C for 1 h. The samples were analyzed by PAGE under denaturating conditions. *Panel A*, wt UvrB; *Panel B*, ΔβhUvrB. *Panel C*, kinetics of the incision reaction.

that ATP binding/hydrolysis is absolutely required for NER (6). In our padlock model (25) we suggest that the formation of a stable UvrB-DNA pre-incision complex requires free energy, which might be available either through ATP hydrolysis by $UvrA_2B$ or as a result of complex formation. To test whether the altered DNA binding properties of ΔβhUvrB are due to an

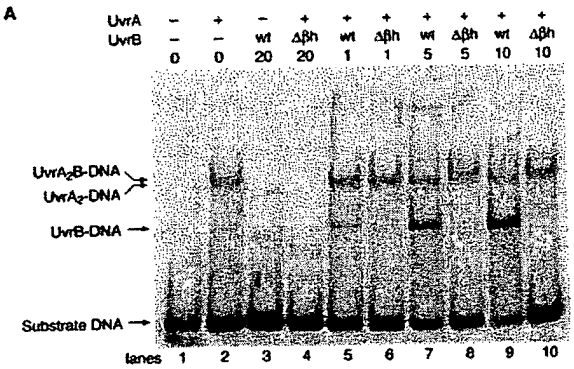

FIG. 4. **Binding of Δβh UvrB to F_{26}-50 dsDNA.** UvrA (20 nM) was incubated with various amounts of wild-type or mutant (Δβh) UvrB as indicated at 55 °C for 20 min in the presence of 2 nM F_{26}-50 duplex DNA with the modified strand 5′ terminally labeled. The reaction mixtures were analyzed on 4% polyacrylamide native gels in the presence of ATP (1 mM) and $MgCl_2$ (10 mM). *Panel A*, lower concentrations of Δβh UvrB (1–10 nM); *panel B*, higher concentrations of Δβh UvrB (50–200 nM).

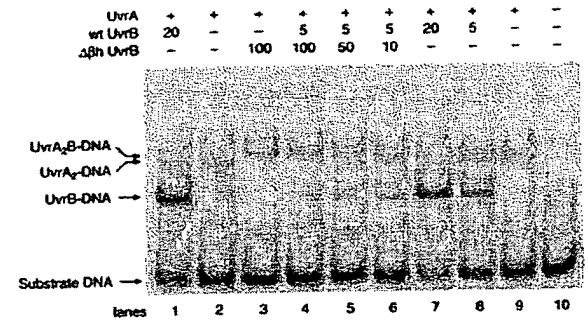

FIG. 5. **Competition between wt and Δβh UvrB in binding to F_{26}-50 dsDNA.** UvrA (20 nM), wt UvrB (5 nM), and increasing amounts of Δβh UvrB (10–100 nM) were incubated at 55 °C for 20 min with 2 nM F_{26}-50 dsDNA. The reaction mixtures were analyzed by 4% native PAGE using Tris-borate-EDTA running buffer with 1 mM ATP and 10 mM $MgCl_2$.

altered ATPase activity, we have examined this activity for both wild type UvrB and Δβh UvrB (Table I). By itself, Δβh UvrB has a very low ATPase activity at 37 °C (2.88 μmol of ATPase/min/mg of protein), similar to wild type UvrB (1.40 μmol/min/mg). In this respect, *B. caldotenax* UvrB resembles *E. coli* UvrB that has a cryptic ATPase activity. It has been shown that full ATPase activity of UvrB requires the presence of both UvrA and DNA (33). Our data show that the ATPase activity of Δβh UvrB is not affected by deletion of the β-hairpin motif. In fact, in the presence of UV-irradiated DNA, the ATPase activity of the $UvrA_2$ ΔβhUvrB complex is higher than that of the $UvrA_2$ wt UvrB complex (29, 22 μmol/min/mg, respectively). This is further evidence that UvrA and Δβh UvrB

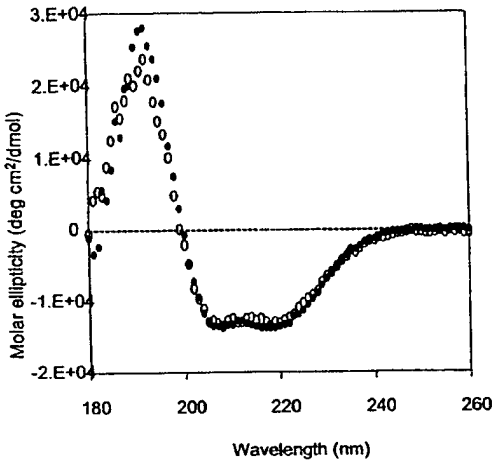

FIG. 6. **CD Spectra of wt and Δβh UvrB.** CD spectra of wt UvrB (*filled circles*) and Δβh UvrB (*open circles*) collected in the range between 180 and 260 nm.

interact, as was suggested from our previous experiments (gel mobility shifts, CD spectra, helicase assay). The deletion of the β-hairpin does not interfere with the ATP hydrolysis by UvrB in the $UvrA_2B$ complex, but apparently the free energy of hydrolysis is not coupled to proper processing of the DNA that is necessary for UvrC binding and incision.

DISCUSSION

Mutational analysis of UvrB has not yet identified which parts of UvrB are involved in DNA binding (reviewed in Ref. 28). One complication is that UvrB has an ATPase activity that is stimulated by DNA binding and is necessary for the formation of the pre-incision complex. Thus, defects of UvrB mutants defective in DNA binding might be due to defects in ATP binding/hydrolysis and vice versa. So far, mutants characterized for both properties showed either inactivation of both or no effect on either. Most of the mutations that affect DNA binding are located in the six highly conserved sequence motifs found in helicases of superfamily I and II. In a previous report (25) we presented a three-dimensional structure of the UvrB protein from the thermophilic bacterium *B. caldotenax*. The crystal structure of *B. caldotenax* UvrB has a significant level of similarity with that of helicase NS3 (34). By superposition of *B. caldotenax* UvrB with the helicase domains of NS3 complexed with DNA, we have hypothesized a model for the UvrB-DNA pre-incision complex, which has a pivotal role in the mechanism of damage recognition by the UvrABC system. In our model we propose a padlock-like binding mode of UvrB to wrap around one DNA strand by inserting a β-hairpin between the two strands of DNA (28).

To test our model and investigate the functional role of the β-hairpin motif, we constructed a β-hairpin deletion mutant (Δβh UvrB) in which residues 97–112 are replaced by a glycine, removing the tip of the β-hairpin. Data presented here show that the β-hairpin deletion mutant 1) is greatly reduced in its ability to support incision, 2) is unable to bind to a damage-containing duplex, 3) cannot destabilize a damage-containing 26-mer, and 4) has retained the ability to hydrolyze ATP in a UvrA and damaged DNA-dependent manner. Thus, functions of UvrB required for the formation of the UvrB-DNA complex, namely UvrA binding and ATP hydrolysis, are not disrupted in the deletion mutant. Nevertheless, Δβh UvrB is unable to form a stable complex with DNA, strongly suggesting that the deleted residues are directly involved in DNA binding.

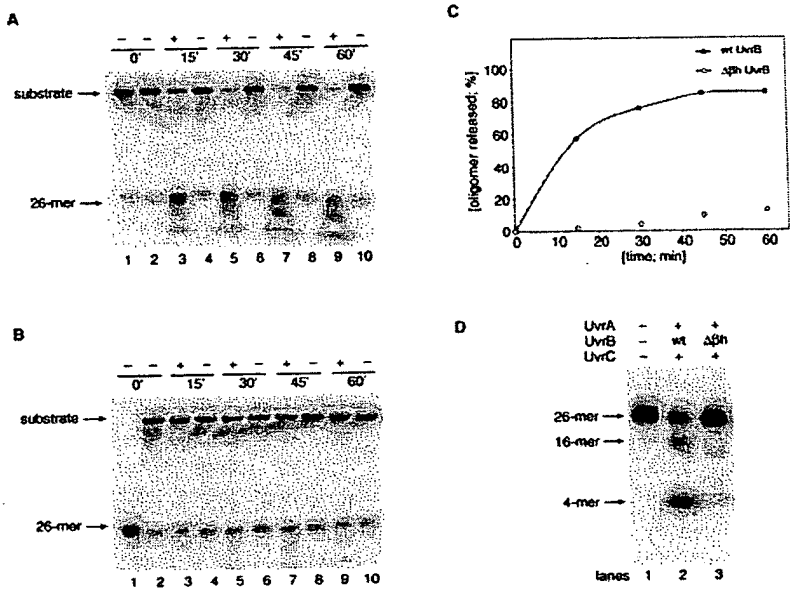

FIG. 7. **ΔβhUvrB is not capable of destabilizing or incising a fluorescein-containing 26-mer annealed to ssHS1F-M13mp19(+) DNA.** For the kinetics of release, HS1F-M13mp19(+) DNA (8 fmol) (sequence shown in Fig. 1*B*, with the modified strand 5′ terminally labeled) was incubated with UvrA (50 nM) and UvrB (100 nM), wt, or Δβh at 37 °C for the indicated periods of time. The reactions were terminated with stop buffer containing SDS, and the reaction mixtures were analyzed by 12% native PAGE. The figure shows the kinetics of 26-mer release by wt UvrB (*panel A*), Δβh UvrB (*panel B*), and graphic comparison of both wt and Δβh UvrB (*panel C*). *Panel D*, incision of a 26-mer containing fluorescein. HS1F-M13mp19(+) DNA (8 fmol) with a 5′ terminally labeled modified strand was incubated with UvrA (20 nM), UvrB (60 nM), and UvrC (50 nM) at 55 °C for 1 h. The samples were analyzed by PAGE under denaturing conditions.

TABLE I
ATPase activity of B. caldotenax UvrA, and UvrB

Samples	ATPase activity
	μmol of ATP hydrolyzed/ μmol of protein/min
UvrA	13.2 ± 0.6
UvrA + UV ϕDNA	17.0 ± 1.0
UvrB	1.4 ± 0.1
UvrB + UV ϕDNA	1.4 ± 0.1
UvrA + UvrB	18.3 ± 1.1
UvrA + UvrB + UV ϕDNA	22.0 ± 0.5
Δβh UvrB	2.8 ± 0.1
UvrA + Δβh UvrB	19.0 ± 0.6
UvrA + Δβh UvrB + UV ϕDNA	29.0 ± 1.0

During the late 1980s and early 1990s Grossman and coworkers developed a "helicase scanning model" of damage recognition (6–8). In this model, $UvrA_2B$ can displace short oligonucleotides and also generate negative and positive supercoiled DNA as it migrates through the helix in search of damage. It was predicted that the helicase machine will stall at a lesion. However, UV was found to stimulate the negative/positive supercoiling, inconsistent with this earlier model (8).

Because of these discrepancies Gordienko and Rupp (11) developed a "damage-processing model" in which damage clearly increased the displacement of oligonucleotides (11). In this model $UvrA_2B$ finds damage by random diffusion. Once a lesion is encountered, the affinity of UvrA for DNA and UvrB is somehow weakened, and the dissociation of UvrA results in a UvrB-DNA complex. The DNA in this complex is greatly distorted, and it is believed that it is this step that requires ATP binding/hydrolysis to allow UvrB to facilitate cleavage upon UvrC binding. It is important to note that although these experiments have described the activity of $UvrA_2B$ as helicase-like, the DNA in these complexes is only destablized and not fully dissociated. In agreement with these results, we show here that the release of the 26-mer containing the damage does not occur until the addition of the loading buffer containing SDS. Because UvrC can still incise the destabilized strand, these results are inconsistent with a true helicase activity in which the strand is fully displaced from the complement strand. Our results in Fig. 7 demonstrate that deletion of the β-hairpin inhibits the helix destabilization step.

The pre-incision complex between UvrB and damaged DNA is a key intermediate in excision repair linking damage recognition to the location of dual incision. Once the pre-incision complex is formed UvrB has to remain bound tightly to the DNA without translocating, ensuring precise incisions by UvrC and subsequent removal of the damaged fragment. In contrast to many non-sequence specific protein-DNA complexes, the UvrB-DNA pre-incision complex does not dissociate at high ionic strength, suggesting a hydrophobic mode of DNA binding. It has been suggested that UvrB might form favorable hydrophobic interactions with aromatic amino acid side chains and the DNA bases; however, this has never been directly determined (35) and awaits the solution of a co-crystal structure.

We hypothesize that there are five critical regions in UvrB that are necessary and sufficient for DNA damage binding and processing: 1) a damage recognition pocket located at the base of the β-hairpin; 2) a flexible β-hairpin, which acts as a padlock to secure the non-damaged strand in place; 3) an ATP binding site, which facilitates conformational changes in UvrB; 4) the coiled-coiled C terminus of UvrB, which interacts with UvrC; and finally, 5) residues in domain 3 that contain helicase motifs IV-VI which help drive a conformational change in the DNA, leading to incision. How might the β-hairpin motif participate in allowing UvrB to bind and process damage? In our padlock DNA binding model of UvrB, the β-hairpin must first open to accept a strand of DNA and then close to lock one DNA strand; we favor the non-damaged strand, forming a stable UvrB-DNA interaction. Taking a closer look at the anatomy of the β-hairpin reveals four critical regions, three of which were removed in the Δβh mutant. The tip of the β-hairpin is hydrophobic in character and interacts with hydrophobic residues in domain Ib. Two salt bridges located in the middle of the hairpin provide further strength to the lock. Preserved in the Δβh mutant is an aromatic base containing several Tyr and Phe residues that are 100% conserved in all bacterial species examined to date. We propose that these residues are part of the damage recognition pocket. However, the interaction energy of these residues with the damaged strand without the strong padlock holding onto the non-damaged strand are apparently insufficient to provide sufficient binding energy in the Δβh mutant for productive

binding (Fig. 4) and incision (Fig. 3). In this regard it is interesting to note that UvrB binds to single-stranded oligonucleotides with a K_d of 0.83–1.5 μM and has an increased affinity for damaged DNA (19, 36). Because all our experiments were performed with UvrB and DNA concentrations well below this K_d, it is not unexpected that we did not see any productive binding or incision.

Having formed a stable UvrB-DNA complex, how is incision achieved? It is believed that UvrC is recruited to the UvrB-DNA complex through a coiled-coiled domain at the C terminus of UvrB. We envision that UvrB uses the closure of domain III through ATP binding and/or hydrolysis to further distort the damaged DNA strand in order to drive the phosphate backbone into the nuclease cleft at the N terminus of the UvrC to initiate the 3′-incision (37). However, the ATPase activity of Δβh UvrB mutant is still active and actually more robust than wild type (Table I), suggesting that futile cycles of ATP hydrolysis occur as the Δβh mutant UvrB attempts to grip and distort the DNA with the remaining stump (lacking the salt bridge and hydrophobic tip, see Fig. 1*B*). We have previously shown that UvrB and UvrC, in the complete absence of UvrA, can in an ATP-dependent manner coordinately incise a DNA bubble-substrate containing a lesion in a 4–6 bases unpaired region (12). Loss of the β-hairpin motif completely abolished this activity (data not shown), further supporting the hypothesis that the β-hairpin is required for productive DNA binding and incision. Finally, these observations taken together suggest that UvrA is required to help open up the DNA strands for insertion of the β-hairpin into the DNA helix, thereby allowing proper juxtaposition of the damage recognition pocket to the site of the DNA lesion.

In summary, our data clearly indicate that the upper part of the β-hairpin (residues 97–112) is absolutely required for DNA damage recognition by the UvrABC system, since the Δβh UvrB failed to bind the damaged DNA, support incision, and had no strand destabilizing activity. These results are simply not due to a large conformational change in Δβh UvrB, since CD experiments indicate that the deletion mutant and wt protein have nearly identical spectra. This is further supported by the ability of the mutant protein to interact with UvrA and demonstrate an ATPase activity that is induced in the presence of UvrA and UV-irradiated DNA (Table I). We are currently studying the importance of the individual amino acid residues within the β-hairpin as well as those residues presumably involved in the formation of salt bridges that might be essential for the proper function of the β-hairpin.

Note Added in Proof—While this paper was in press, Goosen and co-workers (*EMBO J.* **20,** 6140–6149) described three sets of double mutants (Y101+F108; Y95+Y96; Y92+Y93) that also support a direct role of the β-hairpin in damage recognition and DNA binding.

REFERENCES

1. Friedberg, E. C., Walker, G. C., and Siede, W. (1995) *DNA Repair and Mutagenesis*, American Society for Microbiology, Washington, D. C.
2. Sancar, A. (1996) *Annu. Rev. Biochem.* **65,** 43–81
3. Lloyd, R. S., and Van Houten, B. (1995) in *DNA Damage Recognition* (Vos, J.-M., ed) pp. 25–66, R. G. Landes Co., Biomedical Publishers, Austin, TX
4. Van Houten, B. (1990) *Microbiol. Rev.* **54,** 18–51
5. Grossman, L., Lin, C. I., and Ahn, Y. (1998) in *Nucleotide Excision Repair in Escherichia coli* (Nickoloff, J. A., and Hoekstra, M. F., eds) Vol. 1, pp. 11–27, Humana Press Inc., Totowa, NJ
6. Oh, E. Y., and Grossman, L. (1987) *Proc. Natl. Acad. Sci. U. S. A.* **84,** 3638–3642
7. Oh, E. Y., and Grossman, L. (1989) *J. Biol. Chem.* **264,** 1336–1343
8. Koo, H. S., Claassen, L., Grossman, L., and Liu, L. F. (1991) *Proc. Natl. Acad. Sci. U. S. A.* **88,** 1212–1216
9. Orren, D. K., and Sancar, A. (1989) *Proc. Natl. Acad. Sci. U. S. A.* **86,** 5237–5241
10. Orren, D. K., and Sancar, A. (1990) *J. Biol. Chem.* **265,** 15796–15803
11. Gordienko, I., and Rupp, W. D. (1997) *EMBO J.* **16,** 889–895
12. Zou, Y., and Van Houten, B. (1999) *EMBO J.* **18,** 4889–4901
13. Sancar, A., and Rupp, W. D. (1983) *Cell* **33,** 249–260
14. Verhoeven, E. E., van Kesteren, M., Moolenaar, G. F., Visse, R., and Goosen, N. (2000) *J. Biol. Chem.* **275,** 5120–5123
15. Moolenaar, G. F., Franken, K. L. M. C., Dijkstra, D. M., Thomas-Oates, J. E., Visse, R., van de Putte, P., and Goosen, N. (1995) *J. Biol. Chem.* **270,** 30508–30515
16. Moolenaar, G. F., Franken, K. L. M. C., van de Putte, P., and Goosen, N. (1997) *Mutat. Res.* **385,** 195–203
17. Moolenaar, G. F., Herron, M. F., Monaco, V., van der Marel, G. A., van Boom, J. H., Visse, R., and Goosen, N. (2000) *J. Biol. Chem.* **275,** 8044–8050
18. Lin, J. J., and Sancar, A. (1991) *Proc. Natl. Acad. Sci. U. S. A.* **88,** 6824–6828
19. Hsu, D. S., Kim, S.-T., Sun, Q., and Sancar, A. (1995) *J. Biol. Chem.* **270,** 8319–8327
20. Caron, P. R., Kushner, S. R., and Grossman, L. (1985) *Proc. Natl. Acad. Sci. U. S. A.* **82,** 4925–4929
21. Husain, I., Van Houten, B., Thomas, D. C., Abdel-Monem, M., and Sancar, A. (1985) *Proc. Natl. Acad. Sci. U. S. A.* **82,** 6774–6778
22. Orren, D. K., Selby, C. P., Hearst, J. E., and Sancar, A. (1992) *J. Biol. Chem.* **267,** 780–788
23. Moolenaar, G. F., Visse, R., Ortiz-Buysse, M., Goosen, N., and van de Putte, P. (1994) *J. Mol. Biol.* **240,** 294–307
24. Goosen, N., Moolenaar, G. F., Visse, R.,., and van de Putte, P. (1998) in *Nucleic Acids and Molecular Biology* (Eckstein, F., and Lilley, D. M. J., eds) Vol. 12, pp. 103–123, Springer-Verlag, Berlin
25. Theis, K., Chen, P. J., Skorvaga, M., Van Houten, B., and Kisker, C. (1999) *EMBO J.* **18,** 6899–6907
26. Machius, M., Henry, L., Palnitkar, M., and Deisenhofer, J. (1999) *Proc. Natl. Acad. Sci. U. S. A.* **96,** 11717–11722
27. Nakagawa, N., Sugahara, M., Masui, R., Kato, R., Fukuyama, K., and Kuramitsu, S. (1999) *J. Biochem. (Tokyo)* **126,** 986–990
28. Theis, K., Skorvaga, M., Machius, M., Nakagawa, N., Van Houten, B., and Kisker, C. (2000) *Mutat. Res.* **460,** 277–300
29. Sohi, M., Alexandrovich, A., Moolenaar, G., Visse, R., Goosen, N., Vernede, X., Fontecilla-Camps, J. C., Champness, J., and Sanderson, M. R. (2000) *FEBS Lett.* **465,** 161–164
30. Gorbalenya, A. E., Koonin, E. V., Donchenko, A. P., and Blinov, V. M. (1989) *Nucleic Acids Res.* **17,** 4713–4730
31. Soultanas, P., Dillingham, M. S., Velankar, S. S., and Wigley, D. B. (1999) *J. Mol. Biol.* **290,** 137–148
32. Cheetham, G. M., Jeruzalmi, D., and Steitz, T. A. (1999) *Nature* **399,** 80–83
33. Caron, P. R., and Grossman, L. (1988) *Nucleic Acids Res.* **16,** 10891–10902
34. Kim, J. L., Morgenstern, K. A., Griffith, J. P., Dwyer, M. D., Thomson, J. A., Murcko, M. A., Lin, C., and Caron, P. R. (1998) *Structure (Lond.)* **6,** 89–100
35. Van Houten, B., and Snowden, A. (1993) *Bioessays* **15,** 51–59
36. Yamagata, A., Masui, R., Kato, R., Nakagawa, N., Ozaki, H., Sawai, H., Kuramitsu, S., and Fukuyama, K. (2000) *J. Biol. Chem.* **275,** 13235–13242
37. Moolenaar, G. F., Monaco, V., van der Marel, G. A., van Boom, J. H., Visse, R., and Goosen, N. (2000) *J. Biol. Chem.* **275,** 8038–8043
38. Zou, Y., Liu, T. M., Geacintov, N. E., and Van Houten, B. (1995) *Biochemistry* **34,** 13582–13593